Wiley Online Library
Early View publication on www.wileyonlinelibrary.com
(issue and page numbers not yet assigned;
citable using Digital Object Identifier – **DOI**)

Phys. Status Solidi B, 1–7 (2016) / **DOI** 10.1002/pssb.201600629

physica status solidi b
www.pss-b.com
basic solid state physics

Optimization of CVD parameters for graphene synthesis through design of experiments

Remi Papon*[,1], Christel Pierlot[2], Subash Sharma[1], Sachin Maruti Shinde[1], Golap Kalita[1], and Masaki Tanemura[1]

[1] Department of Frontier Materials, Nagoya Institute of Technology, Gokiso-cho, Nagoya 466-8555, Japan
[2] LCOM, Equipe 'Oxydation et formulation', ESA CNRS 8009, ENSCL, BP108, 59652 Villeneuve d'Ascq Cedex, France

Received 20 September 2016, revised 15 November 2016, accepted 16 November 2016
Published online 16 December 2016

Keywords chemical vapor deposition, CVD, epitaxy, graphene, growth optimization

* Corresponding author: e-mail r.papon.518@stn.nitech.jp, Phone: +81 52 735 5276, Fax: +81 52 735 5276

The optimization process of the desired size and quality of graphene domains is usually very difficult due to the numerous interdependent parameters in chemical vapor deposition (CVD). Here, the method so-called "designs of experiments" is applied to estimate the relative importance and value of some of these parameters and their interactions for the CVD growth of graphene on Cu foil using waste plastic as a solid source. We found that the growth temperature, time, rate of heating, and preannealing time of the substrate influence significantly graphene growth. In particular, the growth time and rate of increasing of the carbon source temperature appear as the main factors for the growth of graphene domains, where the manipulation of only these two parameters could dramatically change the size of crystals. Thus, our experiment shows that for synthesis of larger graphene domains using waste plastic not only do the growth parameters of Cu substrate influence graphene growth but also the carbon source rate of heating.

1 Introduction Graphene has attracted a lot of interest due to its exceptional properties, such as optical transparency [1], chemical inertness [2], high carrier mobility (>200 000 $cm^2 V^{-1} s^{-1}$) [1, 3], mechanical strength (>1 TPa) [4] for various device applications. Many methods have been used to obtain graphene, such as mechanical exfoliation, thermal decomposition of SiC [5], reduction of graphene oxide [6], and chemical vapor deposition (CVD). High-quality graphene growth by a CVD technique on transition metals has been recognized as the most feasible and practical approach, especially due to the scalable production of large-area graphene [7–12]. In a CVD process, Cu substrate has been significantly explored due to its low carbon solubility for the growth of monolayer graphene. The graphene films obtained on Cu substrate are generally of polycrystalline nature, which limited graphene optical and electrical properties due to the presence of numerous domain structures and boundaries [13]. In order to achieve the predicted theoretical values of physical and electrical properties, it is essential to increase the size of the graphene domains, thereby reducing defects and domain boundaries. Synthesis of large-sized hexagonal graphene crystals have been reported by using the CVD method [14–17]. In this respect, many precursors have been used for graphene growth on Cu substrate, such as methane [18, 19], ethylene, liquid, and solid precursors [11, 20].

Recently, we have demonstrated that waste plastic can be directly used for graphene growth by the CVD technique. This has enabled us to convert waste plastic to highly value added material. Waste plastic consists of polyethylene and polystyrene, which are composed of linear and ring carbon species. The various carbon species of waste plastic have different melting and boiling points. In this context, various carbon species are produced during the decomposition of waste plastic in a temperature range. In the CVD process, many growth parameters can significantly influence the size of graphene crystals. The optimization of these parameters, step by step, results in a large number of time-consuming experiments. To overcome this, here, we proposed the method called "designs of experiments," which is also

extensively used in organic synthesis [21–23], to establish a clear link between the main parameters and their effects on the synthesis of graphene. The effective experimental process could lead to a better comprehension of the mechanism of growth and structure, and then to an improvement of size of graphene domains.

2 Experimental The experiments were carried out in an atmospheric pressure chemical vapor deposition (AP-CVD) system, with two furnaces and one quartz tube of 4.0 cm diameter and 1.0 m length (Fig. 1a). Details of the experimental system are explained elsewhere [24]. In brief, the growth furnace, with the Cu foil, was first heated to the range of 1050–1070 °C with a gas flow of 100 square cubic centimeters per minute (sccm) of H_2 for the preannealing and annealing to increase the grain size and cleaning of the Cu foil surface. Then, the gases were changed to a mixture of 98 sccm of Ar and 2.5 sccm of H_2 for the graphene growth and cooling down. At the end of the annealing time, the change of gases took 5 min and the carbon source furnace was switched on, making a program with a nucleation point around 415 °C, a decreasing to 390 °C and then the graphene growth with a chosen increasing growth rate, as shown in the temperature profiles (Fig. 1b). The used precursor was a waste polymer, as used before [24, 25]. The domain size and the quality of the synthesized graphene were measured by an optical microscope (VHX-500) and NRS 3300 laser Raman spectrometer with a laser excitation energy of 532.08 nm from a green laser, respectively.

Design of experiments is a method to obtain information with a minimum of experiments with a precision good enough, through a selected mathematical model. For example, the study of five parameters requires $2^5 = 32$ experiments, but due to the aliases between chosen coefficients, it is possible to reduce the number of experiments to $2^3 = 2^{5-2} = 8$ experiments, without reducing the precision of the measurements by too much.

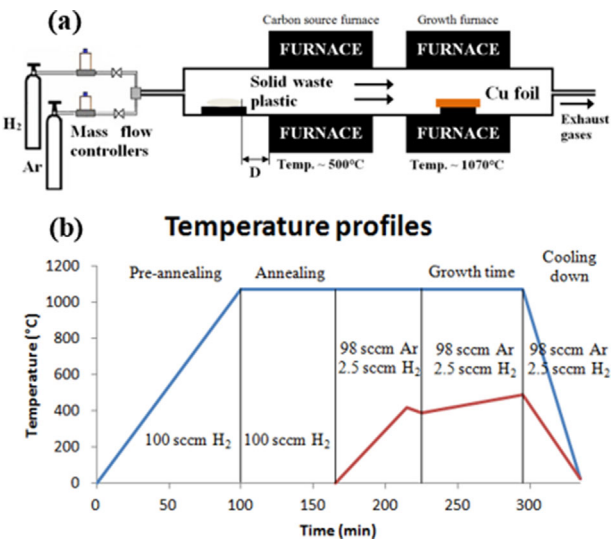

Figure 1 (a) CVD system, (b) temperature profiles on the growth furnace (black square curve) and carbon source furnace (red triangle curve), the indicated times are just an example.

Most of the parameters in this CVD system, such as gas ratios, were fixed throughout the experiments and only six parameters (growth temperature, annealing time, mass of carbon source, rate of increasing of carbon source's temperature ("referred to as rate of heating" hereafter), growth time, distance between the carbon source, and the carbon source furnace [D]) were judged to be the most important in graphene growth and so needed to be optimized in the designs of experiments. We decided to use only five parameters (with four common parameters) in each design of experiments (a 2^{5-2} matrix with two levels due to the numerous parameters, written in Tables 1 and 2, for the design of experiments [DoE] 1 and 2, respectively) due to the upper limit of growth temperature. Indeed, this growth temperature, 1070 °C, is high enough to produce a smooth surface and to avoid too much Cu evaporation and too high a Cu partial pressure that could prevent graphene nucleation [26–29], without melting the Cu. Then, if the first design of experiment (DoE1) has the growth temperature as a parameter, the second (DoE2) studies annealing time instead of growth temperature as a parameter, which is believed to affect Cu surface, especially the size of Cu grains and the removing of impurities [30]. The growth temperature was kept at 1070 °C in DoE2 and the annealing time was 30 min in DoE1.

Furthermore, the four other most important parameters in the CVD synthesis of graphene were the same, but the levels ("level −1" and "level +1" in Tables 1 and 2) were changed, in order to find the best trend of each parameter by comparing the values and results of the two designs of experiments: rate of heating [25], mass of carbon source (waste polymer), growth time [24, 31], and distance (D) between the carbon source furnace and the precursor (carbon source) because the precursor was put outside of the carbon source furnace [24, 25].

The answers, Y_{1a} and Y_{2a}, $a \in [1; 8]$, $a \in \mathbb{N}$, for the experiments of DoE1 and DoE2, respectively (the answers are ranked from Y_{11} to Y_{18} for DoE1, and from Y_{21} to Y_{28} for DoE2), are the average size of graphene crystals (in μm) seen by optical microscope (VHX-500) after slight oxidation of the Cu surface. All calculations of the

Table 1 Parameters of design of experiments 1 (DoE1).

	growth parameters	unit	level −1	level +1
X_{11}	temperature of Cu	°C	1050	1070
X_{12}	rate of increasing	°C mm^{-1}	1.5	2
X_{13}	mass of carbon source	mg	5	8
X_{14}	growth time	min	67	87
X_{15}	distance with the furnace (D)	cm	1	1.5

Table 2 Parameters of design of experiments 2 (DoE2).

	growth parameters	unit	level −1	level +1
X_{21}	annealing time	min	30	60
X_{22}	rate of increasing	$^{\circ}C\,mm^{-1}$	1.2	1.5
X_{23}	growth time	min	90	110
X_{24}	mass of carbon source	mg	3.5	5
X_{25}	distance with the furnace (D)	cm	0.7	1

generators, effects matrices and experiments matrices are presented in the Supporting information (A.1, A.2, and A.3, respectively).

The interactions between the two growth parameters could study the link between these parameters and their influence on the answers, the size of graphene domains.

3 Results and discussion

3.1 Notations In this article, the parameters of each DoE will be written X_{ki}, with $k = \{1, 2\}$, corresponding to DoE1 and DoE2, respectively, and i the values from 1 to 5 (growth parameters of each DoE in Tables 1 and 2). Interactions, between two growth parameters X_{ki} and X_{kj}, are written X_{kij}. X_{10} and X_{20} are the degrees of freedom of the systems, which is not related to any parameter. l_{ki} and l_{kij} are the corresponding coefficients to the parameters X_{ki}. and to the interactions X_{kij}, respectively (the calculations are explained in the Supporting Information B.1). Each parameter has two levels and each level of one parameter has only one value. For example, the value of the level −1 of X_{11} is 1050 °C (Table 1).

3.2 Results of the designs of experiments Each matrix 2^{5-2} proposes eight experiments to build the mathematical models; the experiment matrixes are presented in the Supporting information (Tables SIII and SIV). Then, these 16 experiments were carried out and then 16 answers were measured, Y_{1a} and Y_{2a}, $a \in [1; 8]$, $a \in \mathbb{N}$, for the experiments of DoE1 and DoE2, respectively (the answers are ranked from Y_{11} to Y_{18} for DoE1, and from Y_{21} to Y_{28} for DoE2). The results are presented in Table 3.

In the design of experiments, the parameters with the highest coefficients l_{ki} or l_{kij} in absolute value indicate the most important influences on the final result. In Table 4, the coefficients l_{11}, l_{12}, l_{13}, l_{21}, l_{22}, l_{23}, and l_{24} (in bold letters) are the highest in absolute value and so their

Table 3 The 16 answers Y_{1a} and Y_{2a}, $a \in [1; 8]$, $a \in \mathbb{N}$, from experiments. l_{ki} and l_{kij} are thus calculated through Eqs. (1) and (2), available in the Supporting information, and listed in Table 4.

Y_{11}	Y_{12}	Y_{13}	Y_{14}	Y_{15}	Y_{16}	Y_{17}	Y_{18}
30	35	20	20	25	30	15	20
Y_{21}	Y_{22}	Y_{23}	Y_{24}	Y_{25}	Y_{26}	Y_{27}	y_{28}
25	25	20	20	15	20	10	15

Table 4 Calculated l_{ki} and l_{kij} coefficients through Eqs. (1) and (2).

l_{10}	l_{11}	l_{12}	l_{13}	l_{14}	l_{15}	l_{124}	l_{234}
24.375	**1.875**	**−5.625**	**−1.875**	0.625	0.625	0.625	−0.625
l_{20}	l_{21}	l_{22}	l_{23}	l_{24}	l_{25}	l_{223}	l_{235}
18.75	**1.25**	**−2.5**	**−3.75**	**1.25**	0	0	0

corresponding parameters (X_{11}, X_{12}, X_{13}, X_{21}, X_{22}, X_{23}, and X_{24}) can be considered as the most influent in these designs of experiments. A negative number indicates that the level −1 favors the increase of the answers Y_{1a} and Y_{2a}, $a \in [1; 8]$, $a \in \mathbb{N}$, while a positive number indicates that the level +1 favors the increase of the answer Y_{1a} and Y_{2a}, $a \in [1; 8]$, $a \in \mathbb{N}$. By convention, we write $+X_{ki}$ if the level +1 of X_{ki} favors the answers, $-X_{ki}$ if level −1 of X_{ki} favors the answers and then $X_{ki} = 0$ if the growth parameter has no influence on the system.

Then, the most favorable parameters to increase the answer (size of graphene domains) are: $+X_{11}$, $-X_{12}$, $-X_{13}$, $+X_{21}$, $-X_{22}$, $-X_{23}$, and $+X_{24}$ (Tables 1 and 2).

Thus, DoE1 shows that a higher temperature (1070 °C) ($+X_{11}$), a lower increasing rate (1.5 $^{\circ}C\,min^{-1}$) [$-X_{12}$] and a lower mass of carbon source (5 mg) ($-X_{13}$) are better to grow bigger crystals. In DoE2, a longer annealing time (60 min) [$+X_{21}$], a lower increasing rate (1.2 $^{\circ}C\,min^{-1}$) ($-X_{22}$), a shorter growth time (90 min) ($-X_{23}$), and a higher mass of carbon source (5 mg) ($+X_{24}$) favor bigger crystals.

A higher temperature increases the size of copper domains, while eliminating some impurities, then favors the growth of graphene [26–28]. Longer annealing time also favors a smoother surface of copper [27, 30].

The maximum of carbon source mass found by the comparison of DoE1 and DoE2 seems to indicate that too many adatoms produced by the carbon source with the interaction of H_2 leads to smaller graphene domains, due to too many nucleations and on the other hand, a few adatoms do not allow graphene domains to grow more [26, 21, 32].

The rate of increasing is of major importance, as proven in other experiments [15, 24, 25]. Here, the rate 1.5 $^{\circ}C\,min^{-1}$ is favored of in the DoE1 ($-X_{12}$) and a lower rate of 1.2 $^{\circ}C\,min^{-1}$ is favored in DoE2 ($-X_{22}$). These results suggest that an even lower rate of increasing could still favor a bigger size of graphene in this system.

In DoE2, the shorter growth time of 90 min is preferred ($-X_{23}$), while the difference between 67 and 87 min does not influence the answer much in DoE1 ($l_{14} = 0.625$). This shows that crystals need time to grow, but too long a growth time exposes the crystals to etching [31, 33–35].

3.3 Interactions It is also necessary to study the interactions X_{124} and X_{134} for DoE1, and X_{223} and X_{235} for DoE2, which are made of the average of the two corresponding experiments. For example, in the interaction X_{124}, the values of the answers of the two experiments which

the average is made of are taken according to the values of X_{12} and X_{14} in the effect's matrix of DoE1 (Table SI in the Supporting information): in the corner of level -1 of X_{14} and level $+1$ of X_{12}, the two experiments with the level -1 of X_{14} and level $+1$ of X_{12} inside their parameters give two values of size of graphene domains, 20 and 15, which are Y_{14} and Y_{17}, respectively (in Table 3).

In the interaction X_{124} (Fig. 2), we see clearly that the values for level -1 of X_{12} (30 and 30) are higher than for the level $+1$ of X_{12} (17.5 and 20), then the level -1 of X_{12} favors bigger graphene domains. But, for the level -1 of X_{12}, the levels $+1$ and -1 of X_{14} present the same value (30), showing the little influence of X_{14} here; for the level $+1$ of X_{12}, the value of the level $+1$ of X_{14} (20) is slightly higher than the value of the level -1 of X_{14} (17.5), which indicates that the level $+1$ of X_{14} favors a little the size of graphene domains.

The same way, in the interaction X_{134} (Fig. 3) the level -1 of X_{13} is clearly favorable, along with a small advantage for the level $+1$ of X_{14}, confirming the previous analysis of growth parameters with the l_{ki} ($-X_{12}$, $-X_{13}$, $+X_{14}$).

In the interaction X_{223} (Fig. 4), the level -1 of X_{22} and level -1 of X_{23} are clearly more favorable. In the interaction X_{235} (Fig. 5), the level -1 of X_{23} is favorable, while X_5 has no influence on the system, confirmed by the low coefficient $l_{25} = 0$. Then, the previous analysis of growth parameters with the l_{ki} ($-X_{22}$, $-X_{23}$, $X_{25} = 0$) are confirmed.

3.4 Optimization In order to draw optimized contour curves, the parameters and interactions of the two designs of experiments are optimized and calculated answer for the optimization of the mathematical model are found. The details of the process is explained in the Supporting information (B.1.). The results are available Table 5.

Another writing of these values, for an easier understanding, could be with the different growth times and rates of increasing (Table SV in the Supporting information). Then, these answers can be used as coordinates and the representation with contour curves, through a simulation (details in the Supporting information B.2.), is given in Fig. 6.

The blue contour curves indicate the size of graphene domains. Above 70 min of growth time, the size of graphene domains regularly decreases; more adatoms increase nucleation and then make impossible the growth of large-sized domains. If the growth time is too low, adatoms are not numerous enough and then graphene domains cannot grow.

On the other hand, a higher rate of increasing leads to smaller graphene domains, the number of layers could be controlled [21]: too high a rate of increasing produces enough adatoms to make a second layer, while too low a rate does not permit the growth of the first layer to have large-sized crystals. Thus, there is a most favorable rate of increasing that is clearly shown here by the contour curves,

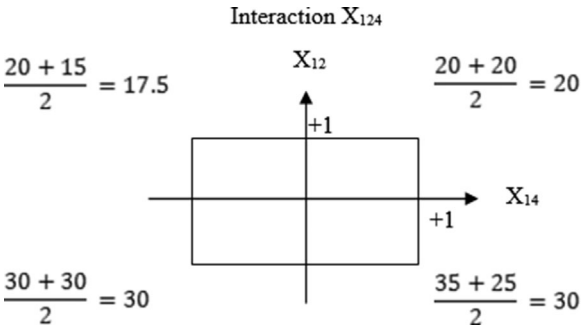

Figure 2 Interaction X_{124} where the most favorable parameters are $-X_{12}$ and $+X_{14}$.

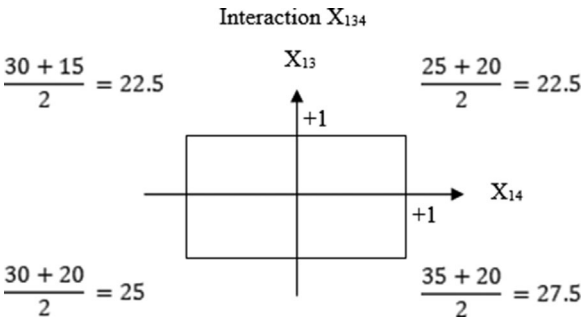

Figure 3 Interaction X_{134} where the most favorable parameters are $-X_{13}$ and $+X_{14}$.

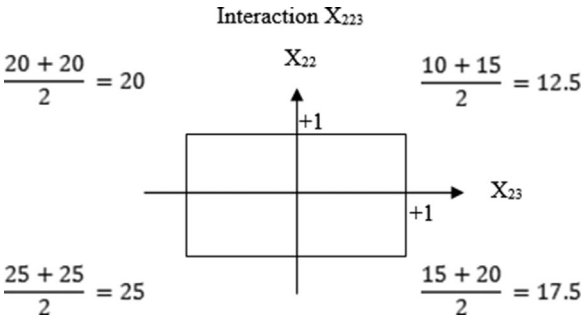

Figure 4 Interaction X_{223} where the most favorable parameters are $-X_{22}$ and $-X_{23}$.

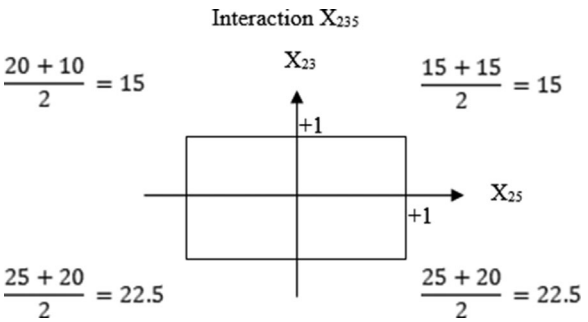

Figure 5 Interaction X_{235} where the most favorable parameters are $-X_{23}$ and $X_{25} = 0$.

Table 5 Calculated answers for the optimization of the mathematical model through Eqs. (6) and (7) in the Supporting Information.

DoE1	$O_{12}=-1$, $O_{14}=-1$ $Y_{1b}=32.5$	$O_{12}=-1$, $O_{14}=1$ $Y_{1c}=33.75$	$O_{12}=$, $O_{14}=-1$ $Y_{1d}=20$	$O_{12}=$, $O_{14}=1$ $Y_{1e}=23.75$	$O_{12}=-0.8$, $O_{14}=-1$ $Y_{1f}=31.25$	$O_{12}=-0.8$, $O_{14}=1$ $Y_{1g}=32.75$
DoE2	$O_{22}=-1$, $O_{23}=-1$ $Y_{2b}=27.5$	$O_{22}=-1$, $O_{23}=1$ $Y_{2c}=20$	$O_{22}=1$, $O_{23}=-1$ $Y_{2d}=22.5$	$O_{22}=1$, $O_{23}=1$ $Y_{2e}=15$	$O_{22}=1.33$, $O_{25}=-1$ $Y_{2f}=21.67$	$O_{22}=1.33$, $O_{23}=1$ $Y_{2g}=14.17$

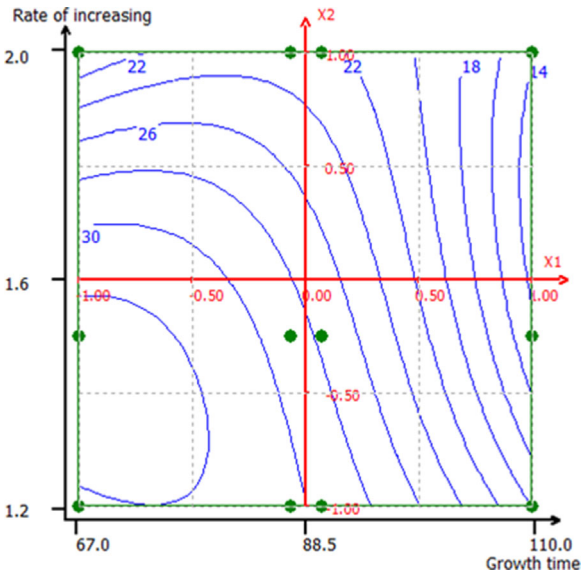

Figure 6 Optimization through contour curves from the mathematical model.

around 1.4 °C min^{-1}. The growth time also shows an optimum around 72 min. These two parameters show an optimum of the size of graphene domains.

3.5 Confirmation Following this finding of an optimum combination of growth time and rate of increasing, an experiment was made with these parameters, including 60 min of annealing, 5 mg of carbon source, a distance of 1 cm, 1.4 °C min^{-1} of rate of increasing, and 72 min of growth time. That gives up to 60 mm graphene domains (Fig. 7), confirming the model. These same optimized conditions on an electropolished Cu substrate give 130 μm crystal (Fig. 8a) with high crystalline structure (Fig. 8b).

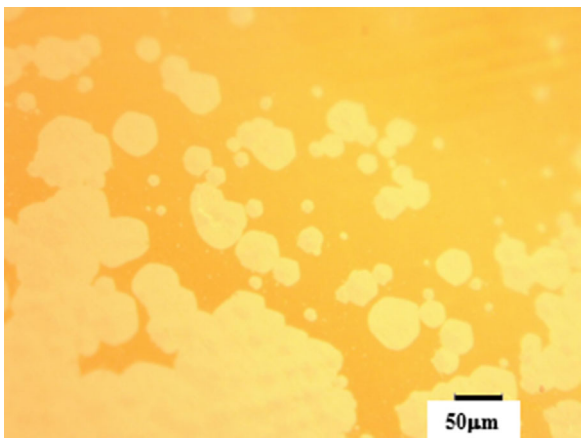

Figure 7 Graphene domains obtained with the best parameters in the two designs of experiments on unelectropolished Cu foil.

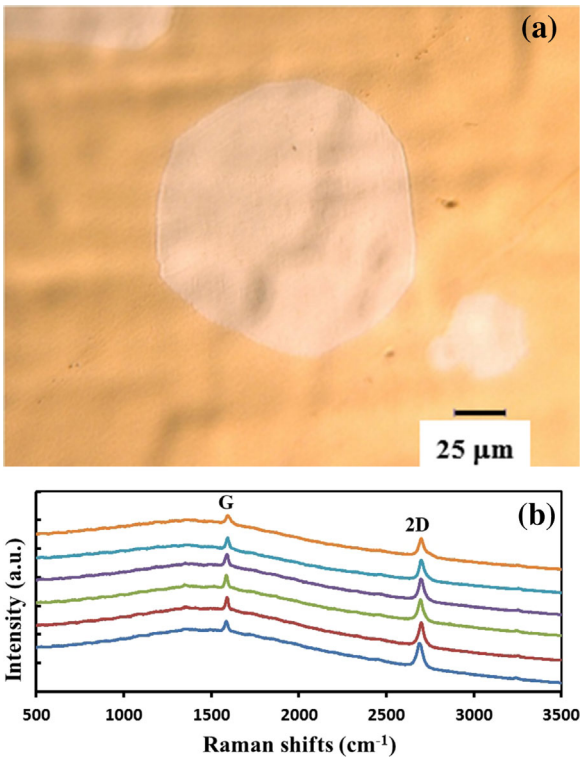

Figure 8 Synthesis on an electropolished Cu foil [29] with optimized parameters determined by the designs of experiments, (a) microscope image of a 130-μm crystal, (b) Raman spectra of the graphene crystals to study the crystalline nature, layer, and defects. Raman spectra at eight randomly selected places show high crystalline structure.

4 Conclusions The two designs of experiments could allow the definition of an optimum quantity of carbon precursor and rate of increasing of the carbon source temperature, along with indications about the growth temperature and growth time. Through the optimization, it was possible to observe a breakthrough in the domain size that implies close interactions between all parameters. In particular, the growth time and rate of increasing of carbon source's temperature appear as main factors in the growth of graphene domains, where the manipulation of only these two parameters could dramatically change the size. The two designs of experiments could allow the definition of an

optimum quantity of carbon precursor and rate of increasing of carbon source's temperature, along with indications about the growth temperature, and growth time. Through the optimization, it was possible to observe a breakthrough in the domain size which implies close interactions between all parameters. In particular, the growth time and rate of increasing of carbon source's temperature appear as main factors to the growth of graphene domains, where the manipulation of only these two parameters could dramatically change the size. The modification of copper surface by electropolishing also leads to an improvement of size of graphene domains, due to the smoother surface and fewer possible nucleation sites.

Supporting Information Additional supporting information may be found in the online version of this article at the publisher's web-site.

Acknowledgement The work is partially supported by Grant-in-Aid for Young Scientists (B) from Japan Society for the Promotion of Science (Grant No. 15K21076).

References

[1] A. K. Geim and K. S. Novoselov, Nature Mater. **6**, 183–191 (2007).
[2] D. Prasai, J. C. Tuberquia, R. R. Harl, G. K. Jennings, B. R. Rogers, and K. I. Bolotin, Graphene: Corrosion-inhibiting coating, ACS Nano. **6**, 1102–1108 (2012).
[3] A. S. Mayorov, R. V. Gorbachev, S. V. Morozov, L. Britnell, R. Jalil, L. A. Ponomarenko, P. Blake, K. S. Novoselov, K. Watanabe, T. Taniguchi, and A. K. Geim, Micrometer-scale ballistic transport in encapsulated graphene at room temperature, Nano Lett. **11**, 2396–2399 (2011).
[4] C. Lee, X. Wei, J. W. Kysar, and J. Hone, Measurement of the elastic properties and intrinsic strength of monolayer graphene, Science **321**, 385–388 (2008).
[5] C. Berger, Z. Song, X. Li, X. Wu, N. Brown, C. Naud et al., Electronic confinement and coherence in patterned epitaxial graphene, Science **312**, 1191–1196 (2006).
[6] S. Stankovich, D. A. Dikin, G. H. Dommett, K. M. Kohlhaas, E. J. Zimney, E. A. Stach et al., Graphene-based composite materials, Nature **442**, 282–286 (2006).
[7] S. Bae, H. Kim, Y. Lee, X. Xu, J.-S. Park, Y. Zheng et al., Roll-to-roll production of 30-inch graphene films for transparent electrodes, Nature Nanotechnol. **5**, 574–578 (2010).
[8] K. S. Kim, Y. Zhao, H. Jang, S. Y. Lee, J. M. Kim, K. S. Kim et al., Large-scale pattern growth of graphene films for stretchable transparent electrodes, Nature **457**, 706–710 (2009).
[9] X. Li, W. Cai, J. An, S. Kim, J. Nah, D. Yang et al., Large-area synthesis of high-quality and uniform graphene films on copper foils, Science **324**, 1312–1314 (2009).
[10] S.-Y. Kwon, C. Ciobanu, V. Petrova, V. Shenoy, J. Bareño, V. Gambin et al., Growth of semiconducting graphene on palladium, Nano Lett. **9**, 3985–3990 (2009).
[11] G. Kalita, M. Masahiro, H. Uchida, K. Wakita, and M. Umeno, Few layers of graphene as transparent electrode from botanical derivative camphor, Mater. Lett. **64**, 2180–2183 (2010).
[12] Y. Lee, S. Bae, H. Jang, S. Jang, S. E. Zhu, S. H. Sim et al., Wafer-scale synthesis and transfer of graphene films, Nano Lett. **10**(2), 490–493 (2010).
[13] D. A. Abanin and L. S. Levitov, Conformal invariance and shape dependent conductance of graphene samples, Phys. Rev. B **78**(3), 035416 (2008).
[14] L. Gao, W. Ren, H. Xu, L. Jin, Z. Wang, T. Ma et al., Repeated growth and bubbling transfer of graphene with millimetre-size single-crystal grains using platinum, Nature Commun. **3**, 699 (2012).
[15] T. Wu, G. Ding, H. Shen, H. Wang, L. Sun, D. Jiang et al., Triggering the continuous growth of graphene toward millimeter-sized grains, Adv. Funct. Mater. **23**(2), 198–203 (2013).
[16] Z. Yan, J. Lin, Z. Peng, Z. Sun, Y. Zhu, L. Li et al., Toward the synthesis of wafer-scale single-crystal graphene on copper foils, ACS Nano **6**, 9110–9117 (2012).
[17] W. Wu, L. A. Jauregui, Z. Su, Z. Liu, J. Bao, Y. P. Chen et al., Growth of single crystal graphene arrays by locally controlling nucleation on polycrystalline Cu using chemical vapor deposition, Adv. Mater. **23**, 4898–4903 (2011).
[18] I. Vlassiouk, P. Fulvio, H. Meyer, N. Lavrik, S. Dai, P. Datskos et al., Large scale atmospheric pressure chemical vapor deposition of graphene, Carbon **54**, 58–67 (2013).
[19] H. Zhou, W. J. Yu, L. Liu, R. Cheng, Y. Chen, X. Huang et al., Chemical vapour deposition growth of large single crystals of monolayer and bilayer graphene, Nature Commun. **4**, 2096 (2013).
[20] Z. Sun, Z. Yan, J. Yao, E. Beitler, Y. Zhu, and J. M. Tour, Growth of graphene from solid carbon sources, Nature **468**, 549–552 (2010).
[21] M. Maiti, V. K. Srivastava, S. Shewale, R. V. Jasra, A. Chavda, and S. Modi, Process parameter optimization through design of experiments in synthesis of high cis-polybutadiene rubber, Chem. Eng. Sci. **107**, 256–265 (2014).
[22] A. Cichocki and P. Koscielniak, Experimental designs applied to hydrothermal synthesis of zeolite ERI+OFF (T) in the Na_2O-K_2O-Al_2O_3-SiO_2-H_2O system Part 2. Regular study, Microporous Mesoporous Mater. **29**, 369–382 (1999).
[23] C. C. Perez, J. M. Pena, and C. R. Duarte Correia, Improved synthesis of bioactive stilbene derivatives applying design of experiments to the Heck–Matsuda reaction, New J. Chem. **38**, 3933 (2014).
[24] S. Sharma, G. Kalita, R. Hirano, S. Shinde, R. Papon, H. Ohtani et al., Synthesis of graphene crystals from solid waste plastic by chemical vapor deposition, Carbon **72**, 6673 (2014).
[25] R. Papon, G. Kalita, S. Sharma, S. Shinde, R. Vishwakarma, and M. Tanemura, Controlling single and few-layer graphene crystals growth in a solid carbon source based chemical vapor deposition, Appl. Phys. Lett. **105**, 133103 (2014).
[26] X. Li, C. Magnuson, A. Venugopal, J. An, J. Suk, B. Han et al., Graphene films with large domain size by a two-step chemical vapor deposition process, Nano Lett. **10**, 4328–4334 (2010).
[27] G. H. Han, F. Güneş, J. J. Bae, E. S. Kim, S. J. Chae, H.-J. Shin et al., Influence of copper morphology in forming nucleation seeds for graphene growth, Nano Lett. **11**, 4144–4148 (2011).
[28] Y. Wu, H. Chou, H. Ji, Q. Wu, S. Chen, W. Jiang et al., Growth mechanism and controlled synthesis of AB-stacked bilayer graphene on Cu-Ni alloy foils, ACS Nano **6**, 7731–7738 (2012).
[29] S. Chen, H. Ji, H. Chou, Q. Li, H. Li, J. W. Suk et al., Millimeter-size single-crystal graphene by suppressing evaporative loss of Cu during low pressure chemical vapor deposition, Adv. Mater. **25**, 2062–2065 (2013).

[30] Y. Jin, B. Hu, Z. Wei, Z. Luo, D. Wei, Y. Xi et al., Roles of H_2 in annealing and growth times of graphene CVD synthesis over copper foil, J. Mater. Chem. A **2**, 16208–16216 (2014).
[31] J. Zhang, P. Hu, X. Wang, and Z. Wang, Structural evolution and growth mechanism of graphene domains on copper foil by ambient pressure chemical vapor deposition, Chem. Phys. Lett. **536**, 123–128 (2012).
[32] C. Wang, W. Chen, C. Han, G. Wang, B. Tang, C. Tang et al., Growth of millimeter-size single crystal graphene on Cu foils by circumfluence chemical vapor deposition, Sci. Rep. **4**, 4537 (2014).
[33] R. Papon, S. Sharma, S. Maruti Shinde, A. Thangaraja, G. Kalita, and M. Tanemura, Formation of graphene nanoribbons and Y-junctions by hydrogen induced anisotropic etching, RSC Adv. **5**, 35301–35297 (2015).
[34] A. Thangaraja, S. Maruti Shinde, G. Kalita, R. Papon, S. Sharma, R. Vishwakarma, K. P. Sharma, and M. Tanemura, Structure dependent hydrogen induced etching features of graphene crystals, Appl. Phys. Lett. **106**, 253106 (2015).
[35] Y. Zhang, Z. Li, P. Kim, L. Zhang, and C. Zhou, Anisotropic hydrogen etching of chemical vapor deposited graphene, ACS Nano **6**(1), 126–132 (2012).